Biochemical and Biophysical Research Communications 446 (2014) 428–433

Contents lists available at ScienceDirect

Biochemical and Biophysical Research Communications

journal homepage: www.elsevier.com/locate/ybbrc

RapGAP9 regulation of the morphogenesis and development in *Dictyostelium*

Hyemin Mun [a,1], Mi-Rae Lee [a], Taeck J. Jeon [a,*]

[a] Department of Biology & BK21 – Plus Research Team for Bioactive Control Technology, College of Natural Sciences, Chosun University, Gwangju 501-759, Republic of Korea

ARTICLE INFO

Article history:
Received 27 January 2014
Available online 7 February 2014

Keywords:
Cytoskeleton
Dictyostelium
Cell adhesion
Cell migration
Cytokinesis

ABSTRACT

Recent reports have demonstrated that the importance of Rap1-specific GTPase-activating proteins (GAPs) in the spatial and temporal regulation of Rap1 activity during cell migration and development in *Dictyostelium*. Here, we identified another putative Rap1 GAP-domain containing protein, showing high sequence homologies with those of human Rap1GAP and *Dictyotelium* RapGAP3, by bioinformatic search. Loss of RapGAP9 resulted in some defects in morphogenesis and development in *Dicytostelium*. *rapGAP9* null cells were more flattened and spread, and highly multinucleated. Compared to wild-type cells, cells lacking RapGAP9 exhibited increased levels of F-actin and more filopodia. These results suggest that RapGAP9 is involved in the regulation of cytoskeleton reorganization and cytokinesis. *rapGAP9* null cells showed a small increase of cell–substratum attachment and slightly lower moving speed and directionality compared to wild-type cells. In addition, the loss of RapGAP9 resulted in an altered morphology of fruiting body with a shorter length of stalk and spore. Identification and characterization of RapGAP9 in this study will provide further insights into the molecular mechanism by which Rap1 regulates cytoskeleton reorganization and morphogenesis in *Dictyostelium*.

1. Introduction

Ras proteins have been the subject of intensive research because of their critical role in human oncogenesis. The *Dictyostelium* Ras GTPase subfamily is comprised of 15 proteins; 11 Ras, 3 Rap, and one Rheb related protein [1]. Rap1 is the closest homolog of the small GTPase Ras and, like Ras, cycles between an inactive GDP-bound and an active GTP-bound conformation. Rap1 activation or deactivation is regulated by guanine nucleotide exchange factors (GEFs) and GTPase-activating proteins (GAPs), respectively [2,3]. The Rap1 protein has an essential function in integrin-mediated cell adhesion and cadherin-mediated cell–cell adhesion [4–6], as well as phagocytosis and cell migration in *Dictyostelium* [7,8]. Recent reports have demonstrated that Rap1 is rapidly and transiently activated in response to chemoattractant stimulation with activity peaking at ~6 s after chemoattractant stimulation and the activated Rap1 localizes at the leading edge of chemotaxing cells [9]. The leading-edge activation of Rap1 regulates cell adhesion and helps establish cell polarity by locally modulating myosin II (MyoII) assembly and disassembly through the Rap1/Phg2 signaling pathway. Spatial and temporal regulation of cell adhesion by Rap1 is required for proper cell migration [9].

RapGAP1 was recently identified as a specific GAP protein for Rap1 and is involved in the temporal and spatial regulation of Rap1 activity in the anterior of chemotaxing cells to control cell–substratum adhesion and MyoII assembly during chemotaxis [9]. RapGAP3 regulates the levels of Rap1 activation during morphogenesis and, by doing so, mediates the proper sorting of prestalk and prespore cells within the multicellular aggregate by controlling cell–cell adhesion and cell migration [10]. To further examine the regulatory functions of Rap1, we previously undertook a bioinformatics search for potential Rap1 GAPs and identified nine open reading frames containing a putative RapGAP domain [9]. In this study, we demonstrate that RapGAP9 is involved in morphogenesis, development, and cell adhesion.

2. Material and methods

2.1. Strains and plasmid construction

Dictyostelium KAx-3 strains were grown in HL5 axenic media or in association with *Klebsiella aerogenes* at 22 °C. The knock-out strains and transformants were maintained in 10 μg/ml blasticidin or

* Corresponding author. Address: College of Natural Sciences Room 3106, Chosun University, Gwangju 501-759, Republic of Korea. Fax: +82 62 230 6654.
E-mail address: tjeon@chosun.ac.kr (T.J. Jeon).
[1] Present address: Asan Institute for Life Science, University of Ulsan College of Medicine, Asan Medical Center, Seoul, Republic of Korea.

http://dx.doi.org/10.1016/j.bbrc.2014.01.196
0006-291X/

20 μg/ml G418. The full coding sequence of the *rapGAP9* was generated by PCR and cloned into the *Eco*RI-*Xho*I site of the expression vector pEXP-4(+) containing a GFP fragment [11]. For expression of truncated RapGAP9 proteins, the various deletion *rapGAP9* sequences were amplified by PCR and cloned into the *Eco*RI-*Xho*I site of a pExp-4(+) vector. We prepared a *rapGAP9* knockout construct by inserting the blasticidin resistance cassette into the *Bam*HI site created at nucleotide 402 of the *rapGAP9* cDNA, and used it for a gene replacement in the KAx-3 parental strains. Randomly selected clones were screened for a gene disruption by PCR.

2.2. Development and chemotaxis analysis

Exponentially growing cells were harvested and washed twice with 12 mM Na/K phosphate buffer (pH 6.1) and plated on Na/K phosphate agar plates at a density of 3.5×10^7 cells/cm^2. The developmental morphology of the cells was examined by photographing the developing cells with a phase-contrast microscope.

The chemotaxis towards cAMP and changes in the subcellular localization of proteins in response to chemoattractant stimulation were examined as described previously [9,12]. The aggregation-competent cells were prepared by incubating the cells at a density of 5×10^6 cells/ml in Na/K phosphate buffer for 10 h. Cell migration was analyzed using Dunn Chemotaxis Chamber (Hawksley). The images of chemotaxing cells were taken at time-lapse intervals of 6 s for 30 min using an inverted microscope. The data were analyzed by using NIS-elements software (Nikon).

2.3. Cell attachment assay

Log-phase growing cells on the plates were washed with Na/K phosphate buffer and resuspended at a density of 2×10^6 cells/ml. The amount of 4×10^5 cells in 200 μl were plated onto 13-mm circular nitrocellulose filters (Millipore). After 30 min, unattached cells were removed by dipping filters into Na/K phosphate buffer. Filters were transferred to microcentrifuge tubes filled with 800 μl Na/K phosphate buffer and vortexed for 1 min with a mixer simultaneously. 150 μl of the detached cells from the filters were plated onto a 30-mm Petri plate with a hole covered by a 0.17-mm glass coverslip, and an additional coverslip was placed on tip. The cells were photographed and counted (detached cell number). To determine the total cell number, 200 μl of the cells was transferred into microcentrifuge tubes filled with 600 μl Na/K buffer and counted. Cell adhesion was presented as a percentage of detached cells compared with total cells. This experiment was repeated three times or more, each time with four filters for each strain.

2.4. DAPI staining

Exponentially growing cells were placed on the coverslip and then fixed with 3.7% formaldehyde for 10 min. The fixed cells were washed with Na/K phosphate buffer, followed by permeabilizing with 0.1% Triton X-100, drying, and then staining with 0.5% Hoechst Dye in 1 ml of mounting solution Fluoromount-G

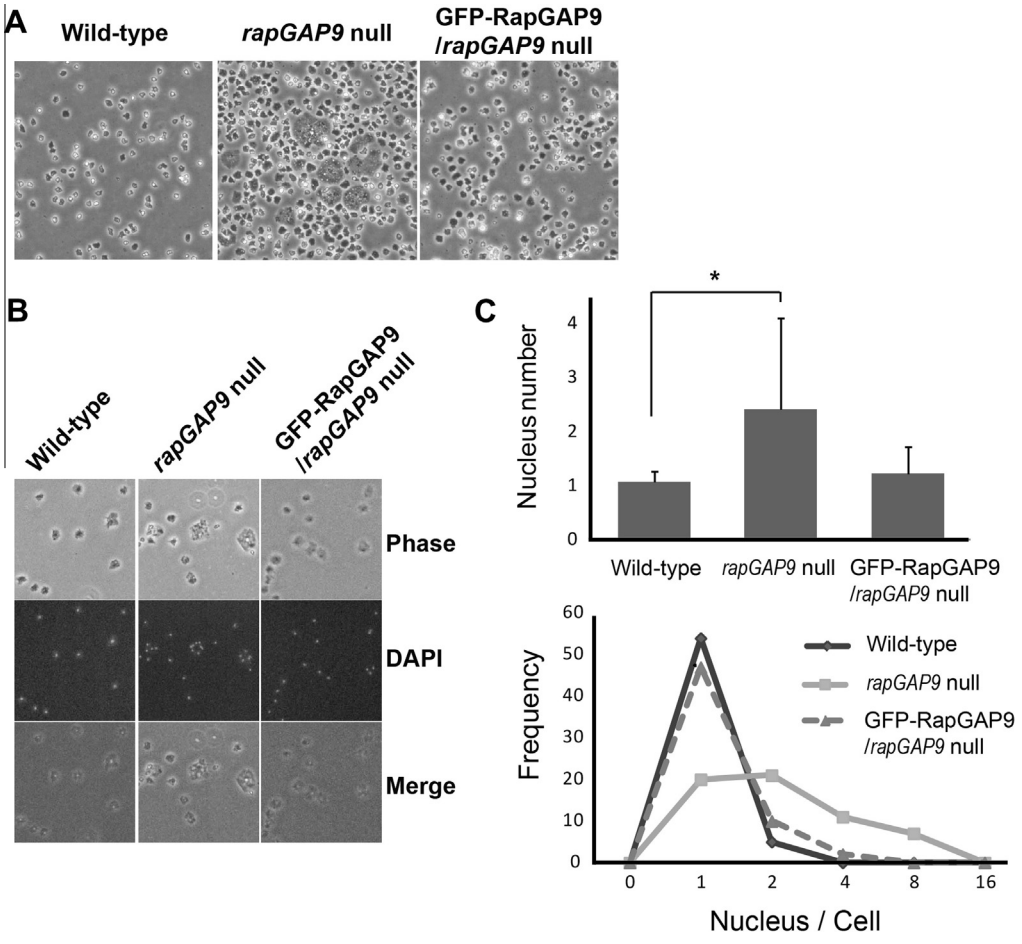

Fig. 1. The cytokinesis defect of *rapGAP9* null cells. (A) Morphology of the cells. Exponentially growing wild-type, *rapGAP9* null cells, and *rapGAP9* null cells expressing GFP-RapGAP9 were photographed. (B) Representative DAPI images of the cells. Corresponding phase-contrast and merged images are shown on the top and bottom panels, respectively. (C) Quantitative analysis of the number of nucleus in the cells. Mean values of the number of nuclei were graphed on the upper part and the frequency distribution was compared on the lower part. Error bars represent SD. Statistically different from control at $^*p < 0.05$ by the student's *t*-test.

(SouthernBiotech). Epifluorescence images of random fields of view were captured by using NIS-elements software (Nikon).

2.5. RT-PCR

The total RNAs from wild-type cells and *rapGAP9* null cells were extracted by using the SV Total RNA Isolation System (Promega), and the cDNAs were synthesized by reverse transcription with MMLV reverse transcriptase (Promega) using random hexamers and 5 μg of total RNAs. 2 μl of the cDNAs were used in the following PCR with 35 cycles employing gene-specific primers. The forward primer tj28 is located at nt 1 to 20 and the reverse primers tj29 and tj30 are located at nt 1084 to 1101 and nt 382 to 399 in cDNA sequence of RapGAP9, respectively. The universal 18S ribosomal RNA specific primers were used as an internal control [9,13].

3. Results

3.1. Identification of the gene encoding RapGAP9 and generation of a *rapGAP9* null cells

To further investigate the pathway leading to Rap1 activation and deactivation, we undertook a bioinformatic search for potential Rap1 GAPs and identified nine proteins with a Rap GAP domain in the *Dictyostelium* genome sequence database. Here we studied a protein of these, referred to as RapGAP9 (DDB0233724). *Dictyostelium* RapGAP9 has 366 amino acids (expected molecular mass 41 kDa) and a GAP domain at the C-terminal region (Fig. S1).

To examine the similarity of RapGAP9 with other GAP domain-containing proteins, the amino acid sequence of the GAP domain of RapGAP9 was compared with those of other GAP proteins by multiple alignments. The GAP domain of RapGAP9 shares 45.8% and 41.1% sequence identities with those of human Rap1GAP and *Dictyostelium* RapGAP3, respectively (Fig. S1). The RapGAP9 GAP domain contains the catalytic Asn251 residue (Asn280 in Hs-RapGAP1) required for Rap1 GAP activity. The phylogenetic trees with *Dictyostelium* RasGAP/RapGAP containing proteins and GAP proteins from other organisms show that RapGAP9 is more closely related to the RapGAP family rather than the RasGAP family (Fig. S1C). These sequence analyses suggest that the GAP domain of RapGAP9 might have GAP activity for Rap1 but not other Ras proteins.

To examine the possible roles of RapGAP9 in cell adhesion, cell motility, and morphogenesis *in vivo*, we created *rapGAP9* null strains (*rapGAP9*⁻ cells) by homologous recombination. The *rapGAP9*

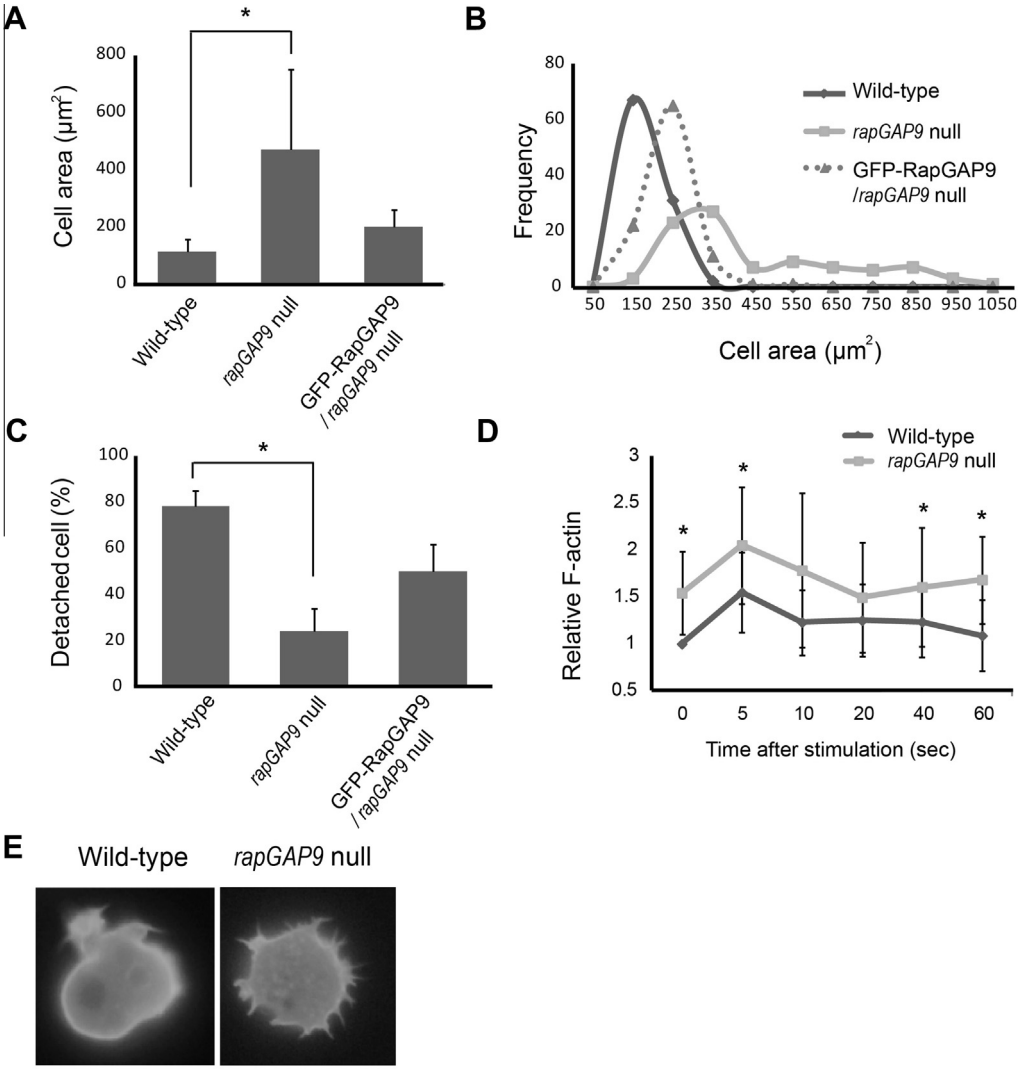

Fig. 2. Cell spreading, cell adhesion and F-actin assembly of *rapGAP9* null cells. (A) Analysis of the cell area. The mean values were graphed. (B) The frequency of the cell area. (C) Cell–substratum adhesion. Adhesion was measured by the ratio of detached cells to the total number of cells. Experiments were performed at least three times. (D) Kinetics of F-actin polymerization in response to chemoattractant stimulation. Error bars represent SD. Statistically different from control at $^{*}p < 0.05$ by the student's *t*-test. (E) Spreading morphology of vegetative cells. Wild-type and *rapGAP9* null cells expressing GFP-ABP were imaged (on the right) to observe the filopodia in the cells.

knockout construct was prepared by inserting the blasticidin resistance cassette into the *rapGAP9* cDNA and used for a gene replacement in KAx-3 parental strains. Randomly selected clones were screened for gene disruption by PCR, and the expression of RapGAP9 in *rapGAP9* null cells was confirmed by RT-PCR (Fig. S2A). The cDNAs were synthesized by reverse transcription with total RNAs extracted from wild-type cells and *rapGAP9* null cells and then used in the PCR using *rapGAP9*-specific primer sets. In the PCR with two sets of primers tj28/tj30 and tj28/tj29, there was no band in *rapGAP9* null cells, whereas a band of approximately 400 bp and 1.1 kb, respectively, in wild-type cells. These data confirm that *rapGAP9* is not expressed in *rapGAP9* null cells. To investigate the roles of RapGAP9 in biological processes, cells overexpressing GFP-RapGAP9 fusion proteins were prepared, and the expression of the protein was confirmed by immunoblotting with anti-GFP antibodies, showing an expected size (68 kDa) of a band (Fig. S2B).

3.2. RapGAP9 is involved in the regulation of morphology and cytokinesis

To address the function of RapGAP9 in cells, we examined the morphology of *rapGAP9* null cells and RapGAP9-overexpressing cells. Compared to wild-type cells, some of *rapGAP9* null cells were more flat and spread out, and highly multinucleated. Examination of the number of nucleus showed that *rapGAP9* null cells have a cytokinesis defect. Majority of wild-type cells contained one nucleus, whereas most of *rapGAP9* null cells had two nuclei and some of the cells over eight nuclei (Fig. 1B and C). The introduction of RapGAP9 into *rapGAP9* null cells rescued the cytokinesis defect of the null cells and the *rapGAP9* null cells expressing RapGAP9 showed normal number of nucleus. These results suggest that RapGAP9 plays an important role in morphogenesis and cytokinesis. Next we measured the size of the cells using NIS-element software. The mean cell size of the *rapGAP9* null cells was approximately 5-fold larger than wild-type cells (Fig. 2A). The morphological phenotype of *rapGAP9* null cells was complemented by expressing RapGAP9, suggesting a function of RapGAP9's on the cell shape formation.

To examine the possible roles of RapGAP9 in cell adhesion, we measured the fraction of cells that detach from a membrane during agitation. *rapGAP9* null cells showed strong attachment compared to wild-type cells and this was partially complemented in GFP-RapGAP9 expressing cells (Fig. 2B). We then investigated the effect of RapGAP9 on chemoattractant-mediated reorganization of the cytoskeleton (Fig. 2C). Wild-type cells exhibited a transient and rapid F-actin polymerization with a peak at 5 s in response to chemoattractant stimulation. The loss of RapGAP9 resulted in 1.5-fold increase in the basal level of F-actin. However, the kinetics of the response was similar to those of wild-type cells with the level of F-actin proportionally higher in *rapGAP9* null cells. In consistent with the increased level of F-actin in *rapGAP9* null cells, when the cells were introduced with F-actin binding protein GFP-ABP, *rapGAP9* null cells displayed more filopodia (Fig. 2D). These data suggest that RapGAP9 is involved in reorganizing the cytoskeleton and cell–substratum attachment.

3.3. RapGAP9 is required for proper cell migration and development

The previous sequence analysis showed the homology of RapGAP9 with RapGAP1 and RapGAP3, which are required for proper cell migration through the regulation of Rap1 activity in

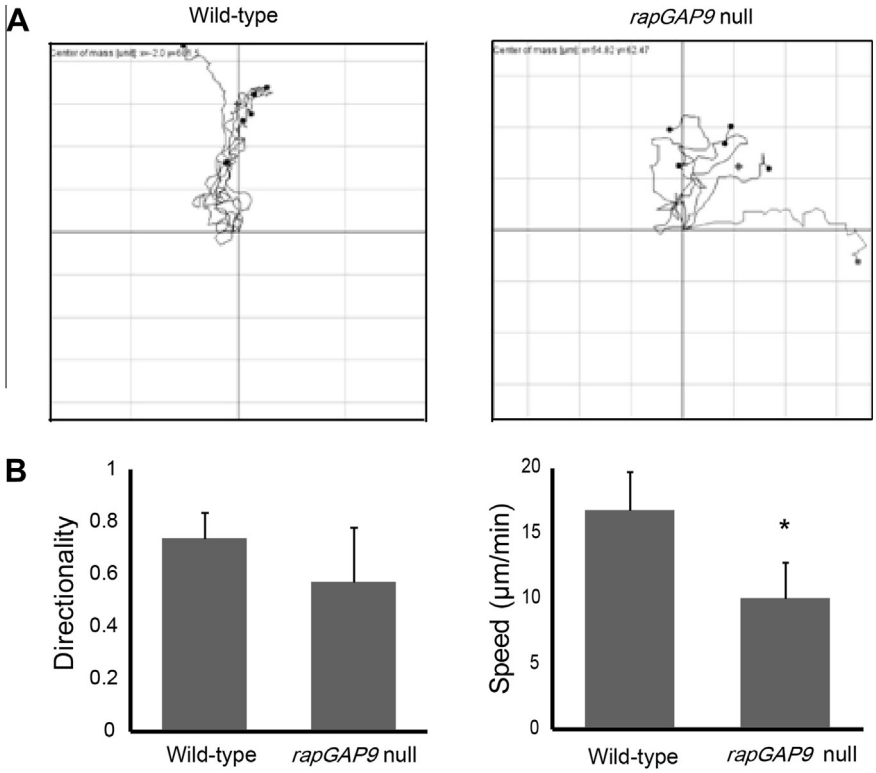

Fig. 3. Chemotaxis of *rapGAP9* null cells. Aggregation-competent cells from wild-type or *rapGAP9* null cells were placed in a Dunn chemotaxis chamber, and the movements of the cells up a chemoattractant (cAMP) gradient were recorded by time lapse photography for 30 min at 6 s intervals. (A) Trajectories of cells migrating toward cAMP in Dunn chemotaxis chamber. Trajectories were tracked with ImageJ software. Each line represents the track of a single cell chemotaxing toward cAMP (150 μM). (B) Analysis of chemotaxing cells. The recorded images were analyzed by NIS-element software. Directionality is a measure of how straight the cells move. Cells moving in a straight line have a directionality of 1.0. It is calculated as the distance moved over the linear distance between the start and the finish. Wild-type cells show a significantly higher directional movement towards an apical region of the organism than *rapGAP9* null cells. Speed indicates the speed of the cell's movement along the total path. Error bars represent SD. Statistically different from control at $^{*}p < 0.05$ by the student's *t*-test.

Dictyostelium [9,10]. In addition, the phenotypes of *rapGAP9* null cells are very similar to those of cells expressing constitutively active Rap1. These data raised a possibility of involvement of RapGAP9 in cell migration and developmental process in *Dictyostelium*. Therefore, we examined the ability of *rapGAP9* null cells to polarize and chemotax up a cAMP chemoattractant gradient using Dunn chemotaxis chamber. *rapGAP9* null cells moved toward a higher concentration of cAMP but the moving speed was slightly lower than that of wild-type cells (Fig. 3). In addition, the directionality, which is a measure of how straight the cells move, of *rapGAP9* null cells was lower than wild-type cells (Fig. 3). These data suggest that RapGAP9 is required for proper cell migration and possibly involved in directional sensing during chemotaxis.

During development in *Dictyostelium*, cells release cAMP, causing surrounding cells to migrate and initiate the formation of a multicellular fruiting body [14]. To examine the possible roles of RapGAP9 in development, we performed a developmental assay. *rapGAP9* null cells aggregated normally to form a mound at ~8 h, with a timing and morphology similar to wild-type cells (Fig. 4A). However, the formation of the fruiting body was slightly delayed in *rapGAP9* null cells, and *rapGAP9* null cells had spores 40% smaller compared to wild type (Fig. 4B). Expression of GFP-RapGAP9 in *rapGAP9* null cells complemented the developmental phenotypes of *rapGAP9* null cells, with developmental timing and morphologies similar to the parental wild-type strain. These results indicate RapGAP9 is required for proper development. The growth rate of the *rapGAP9* null strain was indistinguishable from wild-type cells in suspension (Fig. 4C).

4. Discussion

Our results demonstrate that RapGAP9 is involved in the regulation of morphogenesis and development of *Dictyostelium* cells possibly through controlling reorganization of cytoskeleton. *rapGAP9* null cells showed spread morphology and strong adhesion to the substratum as observed in cells expressing constitutively active Rap1 [9,21]. These phenotypes of *rapGAP9* null cells are observed in cells with high level of Rap1 activity. Cells expressing constitutively active Rap1 or GbpD, which is Rap1-specific GEF protein, and *rapGAP1* null cells displayed flatten shapes and strongly increased cell–substrate attachment [7,1,21], supporting that *rapGAP9* null cells might have a high level of Rap1 activity resulting in spreading morphology and strong adhesion. The putative Rap1 GAP domain of RapGAP9 showed high sequence homology with those of other GAP-domain containing proteins in other organisms. However, RapGAP9 appears to perform some additional functions in

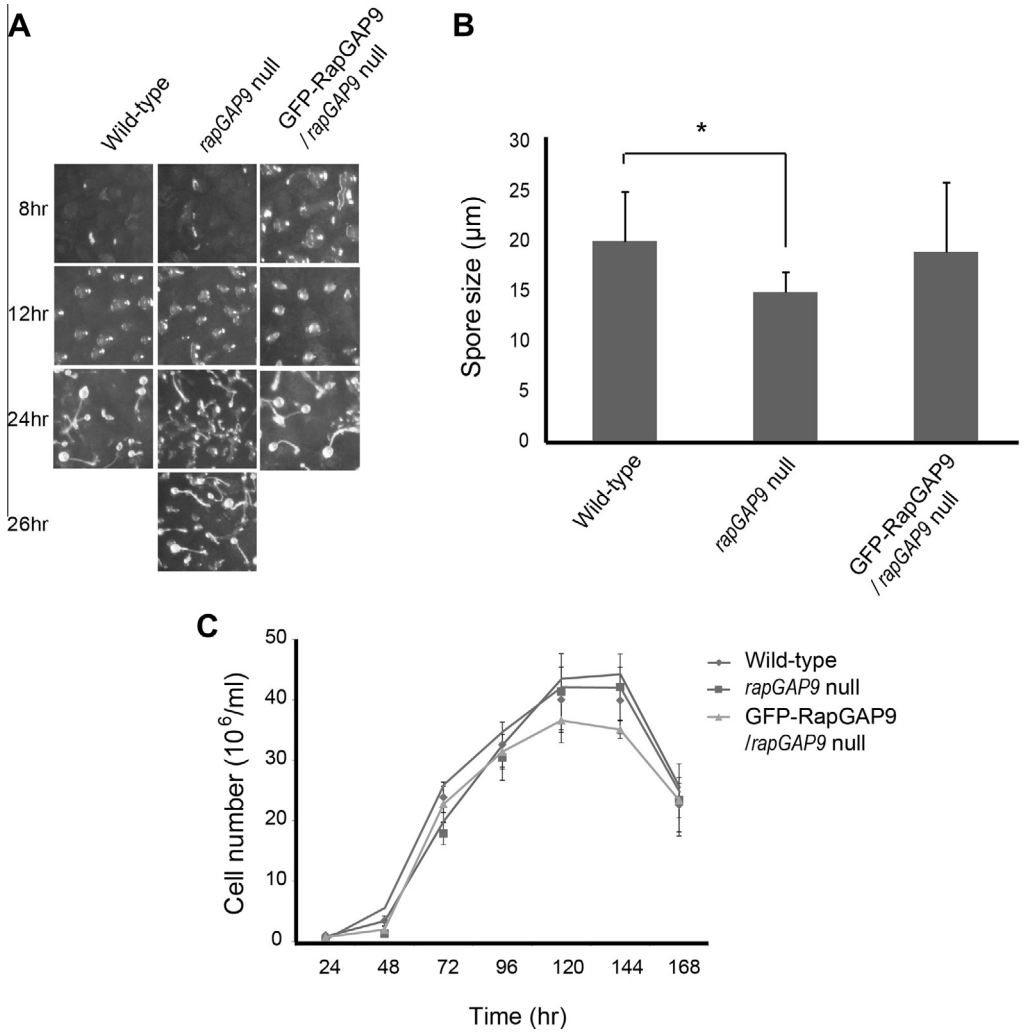

Fig. 4. Development of *rapGAP9* null cells and cells overexpressing RapGAP9. (A) Developmental morphology of *rapGAP9* null cells and cells expressing GFP-RapGAP9. Vegetative cells were washed and plated on non-nutrient agar plates. Photographs were taken at the indicated times after plating. (B) Analysis of the size of the spores at 24 h. *rapGAP9* null cells has smaller spores compared to wild type cells. (C) Growth rates of the cells. KAx-3, *rapGAP9* null, and GFP-RapGAP9/*rapGAP9* null strains were transferred from the growing plates into axenic shaking culture medium and then counted at intervals thereafter. The plotted values are the means of duplicate cell counts. Experiments were performed at least three times. Error bars represent SD. Statistically different from control at $^{*}p < 0.05$ by the student's *t*-test.

cytokinesis and formation of fruiting body. *rapGAP9* null cells were multinucleated and showed smaller size of spores compared to wild – type cells. These phenotypes were not observed in other cells with high level of Rap1 activity such as constitutively active Rap1 or GbpD-overexpressing cells, suggesting a unique function of RapGAP9 in cytokinesis and development independently of Rap1 activity.

RapGAP9 might play some roles in the regulation of cytoskeleton reorganization. Wild-type cells exhibit a biphasic F-actin polymerization profile with a sharp peak at 5 s and a second lower, broader peak linked to pseudopod extension at ~45–60 s [15]. *rapGAP9* null cells exhibited a slightly elevated basal level of F-actin and a proportionally elevated second peak. In support of these data, loss of RapGAP9 caused more filopodia all around the cells and some problems in cell migration with a slightly lower movement speed and directionality compared to wild-type cells. These phenotypes are similar to those of *rapGAP1* null cells or constitutively active Rap1-expressing cells [7,9,21].

Polymerization of the actin cytoskeletal network drives the initial extension of the plasma membrane at the cell front during cell migration. Proteins that regulate actin dynamics and organization, such as vasodilator-stimulated phosphoprotein (VASP), Wiskott–Aldrich syndrome protein (WASP), profilins, and the Arp2/3 complex, localize to the periphery of protruding lamellipodia [22]. GFP-RapGAP9 was observed at the cortex (unpublished data). Upon uniform chemoattractant stimulation, RapGAP9 transiently and rapidly translocated to the cortex and the translocation kinetics of the protein to the cortex in response to chemoattractant stimulation seems to be correlated with F-actin polymerization.

Cytokinesis in eukaryotic organisms is under the intricate control of small GTP-binding proteins of the Ras and Rho families [16–18], even though the underlying molecular mechanisms remained largely elusive. The *Dictyostelium* Ras subfamily comprises 15 proteins. It has been suggested that RasB is involved in cytokinesis. Cells expressing constitutively active RasB have been reported to show abnormal cytokinesis [19]. The phenotype of the *rapGAP9* null cells suggests that RapGAP9 may be involved in cytokinesis. Present studies demonstrate that RapGAP9 plays a crucial role in the formation of the fruiting bodies. RapGAPB and RapGAP3 have been identified to control cell morphology during multicellular development [10,20]. RapGAP1 plays an important role in chemotaxis at the leading edge of moving cells but appears to play no role in development. RapGAP9 is likely to be involved in the late stage of development (Fruiting body formation stage). Further studies would be helpful for understanding the functions of RapGAP9 to determine whether RapGAP9 has GAP activities to Rap1 and other Ras proteins and to examine the expression profile of RapGAP9 during development.

Acknowledgments

This study was supported supported by Basic Science Research Program through the National Research Foundation of Korea (NRF) funded by the Ministry of Education, Science and Technology (2011-0022220), and by research funds from Chosun University to T.J. Jeon, 2011.

Appendix A. Supplementary data

Supplementary data associated with this article can be found, in the online version, at http://dx.doi.org/10.1016/j.bbrc.2014.01.196.

References

[1] A. Kortholt, P.J. van Haastert, Highlighting the role of Ras and Rap during *Dictyostelium* chemotaxis, Cell. Signal. 20 (2008) 1415–1422.
[2] J.L. Bos, Linking Rap to cell adhesion, Curr. Opin. Cell Biol. 17 (2005) 123–128.
[3] J.L. Bos, F.J. Zwartkruis, Signal transduction. Rhapsody in G proteins, Nature 400 (1999) 820–821.
[4] M.R. Kooistra, N. Dube, J.L. Bos, Rap1: a key regulator in cell–cell junction formation, J. Cell Sci. 120 (2007) 17–22.
[5] A. Scrima, C. Thomas, D. Deaconescu, A. Wittinghofer, The Rap-RapGAP complex: GTP hydrolysis without catalytic glutamine and arginine residues, EMBO J. 27 (2008) 1145–1153.
[6] J.H. Raaijmakers, J.L. Bos, Specificity in Ras and Rap signaling, J. Biol. Chem. 284 (2009) 10995–10999.
[7] T.J. Jeon, D.J. Lee, S. Merlot, G. Weeks, R.A. Firtel, Rap1 controls cell adhesion and cell motility through the regulation of myosin II, J. Cell Biol. 176 (2007) 1021–1033.
[8] V. Kolsch, P.G. Charest, R.A. Firtel, The regulation of cell motility and chemotaxis by phospholipid signaling, J. Cell Sci. 121 (2008) 551–559.
[9] T.J. Jeon, D.J. Lee, S. Lee, G. Weeks, R.A. Firtel, Regulation of Rap1 activity by RapGAP1 controls cell adhesion at the front of chemotaxing cells, J. Cell Biol. 179 (2007) 833–843.
[10] T.J. Jeon, S. Lee, G. Weeks, R.A. Firtel, Regulation of *Dictyostelium* morphogenesis by RapGAP3, Dev. Biol. 328 (2009) 210–220.
[11] M.E. Meima, K.E. Weening, P. Schaap, Vectors for expression of proteins with single or combinatorial fluorescent protein and tandem affinity purification tags in *Dictyostelium*, Protein Expr. Purif. 53 (2007) 283–288.
[12] A.T. Sasaki, C. Chun, K. Takeda, R.A. Firtel, Localized Ras signaling at the leading edge regulates PI3K, cell polarity, and directional cell movement, J. Cell Biol. 167 (2004) 505–518.
[13] S. Schroeder, S.H. Kim, W.T. Cheung, K. Sterflinger, C. Breuil, Phylogenetic relationship of Ophiostoma piliferum to other sapstain fungi based on the nuclear rRNA gene, FEMS Microbiol. Lett. 195 (2001) 163–167.
[14] R.L. Chisholm, R.A. Firtel, Insights into morphogenesis from a simple developmental system, Nat. Rev. Mol. Cell Biol. 5 (2004) 531–541.
[15] A.L. Hall, V. Warren, J. Condeelis, Transduction of the chemotactic signal to the actin cytoskeleton of Dictyostelium discoideum, Dev. Biol. 136 (1989) 517–525.
[16] M. Glotzer, The mechanism and control of cytokinesis, Curr. Opin. Cell Biol. 9 (1997) 815–823.
[17] C. Field, R. Li, K. Oegema, Cytokinesis in eukaryotes: a mechanistic comparison, Curr. Opin. Cell Biol. 11 (1999) 68–80.
[18] S.N. Prokopenko, R. Saint, H.J. Bellen, Untying the Gordian knot of cytokinesis. Role of small G proteins and their regulators, J. Cell Biol. 148 (2000) 843–848.
[19] B.W. Sutherland, G.B. Spiegelman, G. Weeks, A Ras subfamily GTPase shows cell cycle-dependent nuclear localization, EMBO Rep. 2 (2001) 1024–1028.
[20] K. Parkinson, P. Bolourani, D. Traynor, N.L. Aldren, R.R. Kay, G. Weeks, C.R. Thompson, Regulation of Rap1 activity is required for differential adhesion, cell-type patterning and morphogenesis in *Dictyostelium*, J. Cell Sci. 122 (2009) 335–344.
[21] M. Lee, T.J. Jeon, Cell migration: regulation of cytoskeleton by Rap1 in Dictyostelium discoideum, J. Microbiol. 34 (2012) 555–561.
[22] A.J. Ridley, M.A. Schwartz, K. Burridge, R.A. Firtel, M.H. Ginsberg, G. Borisy, J.T. Parsons, A.R. Horwitz, Cell migration: integrating signlas from front to back, Science 302 (2003) 1704–1709.